Pergamon

Int. J. Heat Mass Transfer. Vol. 39, No. 3, pp. 537–545, 1996

0017-9310/96 $9.50+0.00

0017–9310(95)00139–5

Linear stability of Couette flow with rotating inner cylinder and radially nonuniform internal heat sources

A. A. KOLYSHKIN

Department of Applied Mathematics, The Riga Technical University, Riga, Latvia 1010

and

RÉMI VAILLANCOURT†

Department of Mathematics and Statistics, University of Ottawa, Ottawa, Ontario, Canada K1N 6N5

(*Received* 7 *October* 1994 *and in final form* 21 *March* 1995)

Abstract—The influence of an axial convective motion caused by radially nonuniform heat sources on the stability of a Couette flow between cylinders, if the inner one is rotating with constant angular velocity and the outer one is fixed, is studied in this paper. The axisymmetric and the first few asymmetric modes are studied. It is found that, for wide gaps, there exist regions of stabilization of Couette flow. These regions, which correspond to asymmetric modes, decrease as the Prandtl number grows.

1. INTRODUCTION

The stability of Couette flow between two rotating cylinders is a classical hydrodynamic problem which has attracted the attention of many researchers since the famous paper by Taylor [1]. The basic stability results are surveyed in [2, 3]. Recently, this problem has been investigated under additional factors such as compressibility of medium, vertical displacement of cylinder walls, axial isothermal flow in the vertical direction, and radially nonuniform temperature distribution in the fluid [4–11] in view of applications to complicated convective heat transfer in thermal systems such as gas turbines and rotating machinery, and new applications such as crystal growth [12] and the design of photochemical reactors for the purification of industrial waste water [8].

A flow between rotating cylinders under radial heating of the fluid is one example of nonisothermal Couette flow. The stability of such flow was initially studied in [13–15], without taking the vertical component of the base velocity of the fluid caused by a nonuniform temperature distribution through the fluid into account. However, experimental studies in [16] indicated that the motion in the vertical direction has an essential influence on the stability and must be taken into account.

A theoretical analysis of the stability of Couette flow under radial heating, where the vertical component of the base velocity is taken into account, is presented in [9], where it is shown that, at certain values of the parameters, a decrease of the Taylor number leads to a sequence of transitions from the axisymmetric mode to asymmetric modes with an increasing number of azimuthal modes. Computational results in [9] compare satisfactorily with experiments [16].

It is known from the analysis of isothermal Couette flow that the finite length of the cylinders greatly influences the flow structure. Nonisothermal Couette flow between two rotating cylinders of finite length, which is affected by the interaction of the density gradient induced by a temperature difference, with a centrifugal force, is studied in [17, 18], where the relative influence of the buoyancy and rotational effects is investigated.

Nonisothermal flow with internal heat sources is another important example for the applications [19, 20]. Such models are used for the analysis of photochemical reactors [21] and in the theory of thermal ignition [22] where an exothermal chemical reaction can lead to convective instability. In some cases (see [23]), nonuniform internal heat sources have to be taken into account in experimental measurements with a laser–Doppler velocimeter. It was found in [23] that the instability of an unsteady circular Couette flow generated by monotonic time-dependent motions of the inner cylinder was initiated near the location where the laser beams penetrated the flow field. Thus, laser beams affect the stability of the flow and this effect was eliminated in [23] by the experiment design.

A theoretical investigation of the stability of a con-

† Author to whom correspondence should be addressed.

NOMENCLATURE

$c = \Im(\lambda)/(kGrv_{0\max})$ phase velocity
c_p constant heat capacity
g acceleration due to gravity
$Gr = g\beta Q_0 h^5/(2\nu^2\kappa\rho c_p)$ Grashof number
$h = (R_2 - R_1)/2$ measure of length
h^2/ν measure of time
k wave number in vertical direction
n wave number in azimuthal direction
$Pr = \nu/\kappa$ Prandtl number
Q volumic density of heat sources
Q_0 constant
$Q_0 h^2/(2\kappa\rho c_p)$ measure of temperature
r radial coordinate
$r_1 = \eta/(1-\eta)$ dimensionless radius of inner cylinder
$r_2 = 1/(1-\eta)$ dimensionless radius of outer cylinder
R_1 radius of inner cylinder
R_2 radius of outer cylinder
$S = \omega R_1/u_0$ parameter
t time
T temperature
$Ta = 64\omega^2 h^4\eta^4/(\nu^2(1-\eta^2))$ Taylor number
$u_0 = g\beta Q_0 h^4/(2\nu\kappa\rho c_p)$ measure of vertical and radial velocity components
$v_{0\max}$ maximum value of vertical component of base velocity
v_r radial velocity component
v_z vertical velocity component
v_φ azimuthal velocity component
z vertical coordinate.

Greek symbols
α parameter characterizing the nonuniformity of heat sources
β thermal expansion coefficient
$\eta = R_1/R_2$ radius ratio
κ thermal conductivity
λ eigenvalue
ν kinematic viscosity
ρ fluid density
φ azimuthal coordinate
ω angular velocity of inner cylinder.

vective motion caused by internal heat sources uniformly, or nonuniformly, distributed through the fluid was done in [24–28]. The influence of an axial convective motion, caused by uniformly distributed internal heat sources, on the stability of a circular Couette flow between two rotating cylinders is studied in [29], where Ta should be corrected as per the remark in parentheses after (20) below.

In the present paper, the stability of a Couette flow with nonuniform heat sources is studied in the region between an inner rotating cylinder and an outer cylinder at rest. Both the axisymmetric (toroidal) and the asymmetric (spiral) modes are studied for different values of the free parameters of the problem.

2. THE MATHEMATICAL ANALYSIS

We consider an infinitely long vertical annular channel of radii R_1 and $R_2 (R_1 < R_2)$. The inner cylinder rotates with constant angular velocity, ω, and the outer cylinder is at rest. The channel is filled with a viscous incompressible fluid. The temperature of both cylinders is constant and equal. We introduce a system of cylindrical polar coordinates $(\tilde{r}, \varphi, \tilde{z})$ with the origin on the axis of the cylinders. The $\tilde{z}$-axis is directed upwards (opposite to gravity) and coincides with the cylinders' axes. The following dimensionless variables (where tilde means a variable with dimension) are used:

$$r = \frac{\tilde{r}}{h} \quad t = \frac{\tilde{t}\nu}{h^2} \quad v_r = \frac{\tilde{v}_r}{g\beta Q_0 h^4/(2\nu\kappa\rho c_p)}$$

$$v_z = \frac{\tilde{v}_z}{g\beta Q_0 h^4/(2\nu\kappa\rho c_p)} \quad v_\varphi = \frac{\tilde{v}_\varphi}{\omega R_1}$$

$$T = \frac{\tilde{T}}{Q_0 h^2/(2\kappa\rho c_p)} \quad p = \frac{\tilde{p}}{g\beta Q_0 h^3/(2\kappa c_p)}$$

where $h = (R_2 - R_1)/2$.

Heat sources of volume density

$$Q(r) = Q_0\, e^{-\alpha(r-r_1)} \tag{1}$$

are distributed within the fluid, where Q_0 and α are constants, $r_1 \leqslant r \leqslant r_2$ and r_1 and r_2 are the dimensionless radii of the cylinders.

The distribution (1) may be caused by a radially radiant source, uniform in the azimuthal and axial directions, inside the inner cylinder. A distribution similar to (1) is used to describe processes in photochemical reactors (see e.g. [21]).

In dimensionless variables, the equations of thermal convection in the Boussinesq approximation are

$$\frac{\partial v_r}{\partial t} + Gr\left(v_r\frac{\partial v_r}{\partial r} + S\frac{v_\varphi}{r}\frac{\partial v_r}{\partial \varphi} + v_z\frac{\partial v_r}{\partial z} - S^2\frac{v_\varphi^2}{r}\right) = -\frac{\partial p}{\partial r} + \nabla^2 v_r - \frac{v_r}{r^2} - S\frac{2}{r^2}\frac{\partial v_\varphi}{\partial \varphi} \tag{2}$$

$$S\frac{\partial v_\varphi}{\partial t} + GrS\left(v_r\frac{\partial v_\varphi}{\partial r} + S\frac{v_\varphi}{r}\frac{\partial v_\varphi}{\partial \varphi} + v_z\frac{\partial v_\varphi}{\partial z} + \frac{v_r v_\varphi}{r}\right) = -\frac{1}{r}\frac{\partial p}{\partial \varphi} + S\nabla^2 v_\varphi - S\frac{v_\varphi}{r^2} + \frac{2}{r^2}\frac{\partial v_r}{\partial \varphi} \tag{3}$$

$$\frac{\partial v_z}{\partial t}+Gr\left(v_r\frac{\partial v_z}{\partial r}+S\frac{v_\varphi}{r}\frac{\partial v_z}{\partial \varphi}+v_z\frac{\partial v_z}{\partial z}\right)=-\frac{\partial p}{\partial z}+\nabla^2 v_z+T \quad (4)$$

$$\frac{\partial T}{\partial t}+Gr\left(v_r\frac{\partial T}{\partial r}+S\frac{v_\varphi}{r}\frac{\partial T}{\partial \varphi}+v_z\frac{\partial T}{\partial z}\right)=\frac{1}{Pr}\nabla^2 T+\frac{2}{Pr}\mathrm{e}^{-\alpha(r-r_1)} \quad (5)$$

$$\frac{\partial v_r}{\partial r}+\frac{v_r}{r}+S\frac{1}{r}\frac{\partial v_\varphi}{\partial \varphi}+\frac{\partial v_z}{\partial z}=0 \quad (6)$$

where

$$\nabla^2=\frac{\partial^2}{\partial r^2}+\frac{1}{r}\frac{\partial}{\partial r}+\frac{1}{r^2}\frac{\partial^2}{\partial \varphi^2}+\frac{\partial^2}{\partial z^2}.$$

Equations (2)–(6) have a steady solution of the following form:

$$v_r=0 \quad v_\varphi=V_0(r) \quad v_z=W_0(r)$$
$$T=T_0(r) \quad p_0(r,z)=p_{01}(z)+p_{02}(r). \quad (7)$$

In practice, we may assume that the channel is closed so that the fluid flux is equal to zero through any cross-section of the channel, that is,

$$\int_{r_1}^{r_2} rW_0(r)\,\mathrm{d}r=0. \quad (8)$$

The boundary conditions are

$$V_0|_{r=r_1}=1,\quad V_0|_{r=r_2}=0,\quad W_0|_{r=r_i}=0,$$
$$T_0|_{r=r_i}=0,\quad i=1,2. \quad (9)$$

The solution to equations (2)–(9) has the form

$$T_0(r)=C_1\ln r+C_2+A(r)+B(r) \quad (10)$$

$$V_0(r)=\frac{r_1r_2^2}{(r_2^2-r_1^2)r}-\frac{r_1 r}{r_2^2-r_1^2} \quad (11)$$

$$W_0(r)=C_3\ln r+C_4+C_5r^2+\int_{r_1}^{r}\left\{\xi\ln\frac{\xi}{r}[C_1\ln\xi+C_2+A(\xi)]-2\xi\ln\xi\,\mathrm{e}^{-\alpha(\xi-r_1)}\times\left(\frac{\xi^2}{2}\ln\frac{\xi}{r}+\frac{r^2-\xi^2}{4}\right)\right\}\mathrm{d}\xi \quad (12)$$

where the constants C_1–C_5 and the functions $A(r)$ and $B(r)$ are given in [28].

The formula for the pressure is omitted since it is not used in the sequel.

We consider the stability of the flow (7), (10)–(12) by the method of normal perturbations. The solutions to problem (2)–(6) in a neighborhood of the base flow (10)–(12) are sought in the form

$$\begin{bmatrix} v_r\\ v_\varphi\\ v_z\\ T\\ p\end{bmatrix}=\begin{bmatrix}0\\ V_0(r)\\ W_0(r)\\ T_0(r)\\ p_0(r,z)\end{bmatrix}+\begin{bmatrix}u(r)\\ v(r)\\ w(r)\\ \theta(r)\\ q(r)\end{bmatrix}\mathrm{e}^{-\lambda t+ikz+in\varphi} \quad (13)$$

where $n=0$ and $n\neq 0$ correspond to toroidal and spiral disturbances, respectively. Substituting equation (13) into (2)–(6) and linearizing the equations in a neighborhood of the base flow (7), (10)–(12), we obtain the following system of equations

$$-\lambda u+Gr\left(S\frac{V_0}{r}inu+W_0iku-S^2\frac{2}{r}vV_0\right)=-\frac{\mathrm{d}q}{\mathrm{d}r}+Lu-\frac{u}{r^2}-inS\frac{2}{r^2}v \quad (14)$$

$$-\lambda v+Gr\left(u\frac{\mathrm{d}V_0}{\mathrm{d}r}+S\frac{V_0}{r}inv+W_0ikv+\frac{u}{r}V_0\right)=-\frac{1}{S}\frac{inq}{r}+Lv-\frac{v}{r^2}+\frac{in}{S}\frac{2}{r^2}u \quad (15)$$

$$-\lambda w+Gr\left(uW_0'+S\frac{V_0}{r}inw+W_0ikw\right)=-ikq+Lw+\theta \quad (16)$$

$$-\lambda Pr\theta+GrPr\left(uT_0'+S\frac{V_0}{r}in\theta+W_0ik\theta\right)=L\theta \quad (17)$$

$$u'+\frac{u}{r}+S\frac{inv}{r}+ikw=0 \quad (18)$$

where

$$L:=\frac{\mathrm{d}^2}{\mathrm{d}r^2}+\frac{1}{r}\frac{\mathrm{d}}{\mathrm{d}r}-\frac{n^2}{r^2}-k^2.$$

The boundary conditions are

$$u|_{r=r_i}=0 \quad v|_{r=r_i}=0 \quad w|_{r=r_i}=0 \quad \theta|_{r=r_i}=0$$
$$i=1,2. \quad (19)$$

The boundary value problem given by equations (14)–(19) is solved by the pseudospectral collocation method. The details of the numerical procedure are given in [27, 30].

The stability of the flow (7), (10)–(12) is determined by the eigenvalues, $\lambda_m=a_m+ib_m$, of problem (14)–(19). If $a_m>0$ for all m, then the flow is stable, and if $a_m<0$, for at least one m, then the flow is unstable.

Two IMSL routines were used, namely: QDAG to compute the integrals in equations (10) and (12), and GVLCG to solve the generalized eigenvalue problem which is obtained from equations (14)–(19) after discretization.

The computer code was tested by comparing our results with results of other authors in the following two particular cases:

(1) isothermal Couette flow [15] and

(2) pure convection with internal heat generation without rotation [25].

In the first case, the computed critical Taylor numbers for different values of $\eta = R_1/R_2$, from 0.1 to 0.95, differ by at most 0.08% from the values given in [15]. In the second case, the computed critical Grashof numbers for $\eta = 0.95$ differ by at most 0.3% from the values given in [25].

3. NUMERICAL RESULTS AND DISCUSSION

Computational results are given in terms of the Taylor number

$$Ta = \frac{64\omega^2 h^4 \eta^4}{\nu^2(1-\eta^2)} \tag{20}$$

for an easy comparison with the results for the isothermal case [15] (in the definition of Ta given in [29], p. 3139, the dimensionless number R^2 in the numerator should be changed to R^4, which corresponds to η^4 in the present paper). The parameter S is related to Ta and Gr by the formula

$$S = \frac{1}{4\eta Gr}\sqrt{\left(\frac{1+\eta}{1-\eta}Ta\right)}. \tag{21}$$

Computations were done for two values of the radius ratio, namely $\eta = 0.7$ and $\eta = 0.4$, three values of the parameter α (which describes the nonuniformity of the heat sources), namely $\alpha = 0$, 0.5, 2, and three values of the Prandtl number, namely $Pr = 1$, 5, 20, since the importance of the Prandtl number on stability characteristics is known [25, 31]. The axisymmetric and the first two asymmetric modes, with azimuthal wave numbers $n = 0, 1, 2$, respectively, were studied. In one case, comparison is made with the modes $n = 3$ and 4.

It is noted that the shape of the neutral stability curves changes considerably if some parameters of the problem are changed. We consider several samples of neutral stability curves.

Figure 1(a) shows four curves which correspond to the axisymmetric mode ($n = 0$) with $\alpha = 0.5$, $Pr = 1$, $\eta = 0.7$. Each curve has only one minimum. The coordinates of the minimum correspond to the critical values of the parameters Gr and k, respectively. Computations show that rotation has a destabilizing effect on the flow; thus the critical Grashof number decreases as the Taylor number grows. Instability in this case is of hydrodynamical nature (sometimes called *thermal-shear instability* [31]) since the role of thermal factors is relatively small for small Prandtl numbers and the energy is transmitted to the perturbations basically from the main flow.

When $\eta = 0.7$, it is known that the classical isothermal Couette flow is unstable at $k_c = 1.57$,

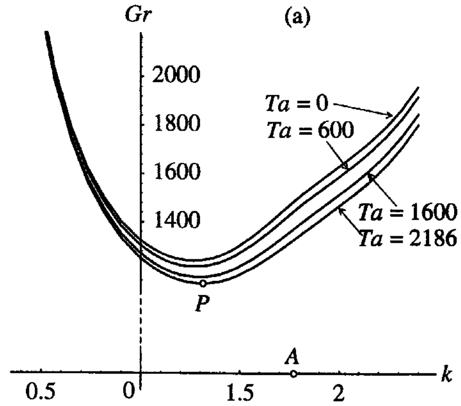

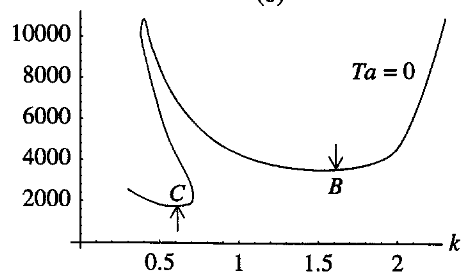

Fig. 1. Neutral stability curves: (a) for $n = 0$ with $Pr = 1$, $\eta = 0.7$, $\alpha = 0.5$ and four values of Ta; (b) for $n = 2$ with $Pr = 5$, $\eta = 0.4$, $\alpha = 2$ and $Ta = 0$.

$Ta_c = 2186$ (see [15]). In this case, $Gr_c = 0$; thus the point A: $(k_c, Gr_c, Ta_c) = (1.57, 0, 2186)$ lies on the k-axis in the (k, Gr)-plane. One would expect that if the Taylor number grew from 0 to Ta_c then the Grashof number would decrease monotonically to 0 and the neutral curve at $Ta = Ta_c$ would be tangent to the k-axis at A. We shall see, later, that such a *continuous transition* to isothermal Couette flow occurs at larger Prandtl numbers. However, for the parameter values used in Fig. 1(a), our computations show that the limit position of the neutral stability curve is reached as Ta increases to the limiting value $Ta_c = 2186$; but Gr decreases only to the limiting value $Gr_* = 1147.9$, and not to zero.

Hence, the stability boundary can be described as follows. If $Ta < Ta_c$, stability is determined by the convective mode associated with the convective flow in the vertical direction [see the curves in Fig. 1(a)]. When $Ta > Ta_c$, the flow is unstable with respect to the pure centrifugal mode for any $Gr > 0$. This situation resembles the uniform heat generation treated in detail in [29]. Therefore a small increase of the Taylor number beyond $Ta = Ta_c$ produces a 'jump' from point P: $(k_*, Gr_*, Ta_c) = (1.31, 1147.9, 2186)$ to point A, that is, a *discontinuous transition* to isothermal Couette flow. We note that such abrupt transition from one regime to another is observed in [32] for $Pr = 1$ where convection is studied in a region between two horizontal rotating cylinders. It is found in [32] that if the Rayleigh number exceeds some value then hysteresis effects are observed, that is, the characteristics of the flow depend considerably on the direction in which the parameters vary.

Figure 1(b) shows a typical curve corresponding to the case $n = 2$, $Pr = 5$, $\eta = 0.4$, $\alpha = 2$, $Ta = 0$. This curve has two minima (points B and C) and one cusp. In general, the curve can have a cusp or a closed loop (or even several closed loops; see, for example, [25, 26]). An elegant physical interpretation of the occurrence of a cusp or loops as the Prandtl number grows is given in [25]. For small Prandtl numbers, the neutral stability curves have the typical shape shown in Fig. 1(a). These curves undergo a continuous deformation as Pr grows. Such a resulting curve is shown in Fig. 1(b) for $Pr = 5$.

The right minimum (point B) corresponds to thermal-shear instability, that is, instability due to the interaction of convective flows moving in opposite directions. Computations show that the position of B does not change considerably as the Prandtl number grows; hence, this minimum can be associated with thermal-shear instability. However, a second minimum (point C) appears as the result of deformation of the neutral curve; in this case C corresponds to the absolute minimum of the neutral stability curve. This minimum is shifted to the region of smaller k and the critical Grashof number decreases. Perturbations in the form of thermal running waves moving downstream with high phase velocity correspond to the lower part of the neutral curve in Fig. 1(b); hence, this minimum can be associated with thermal-buoyant instability. Therefore, depending on the Prandtl number, two kinds of instability can occur: thermal-shear instability and the instability in the form of thermal running waves (thermal-buoyant instability).

If the Taylor number changes, our computations show that, in some cases, a deformation of a neutral curve takes place in the direction indicated by the arrows in Fig. 1(b). This explains 'jump' transitions to different wave numbers (see e.g. [29] and the results given below). Physically, this means that the rotating cells change vertical size. Note that this phenomenon was also observed for Couette flow with radial heating [9].

Figure 2 shows stability curves for the axisymmetric

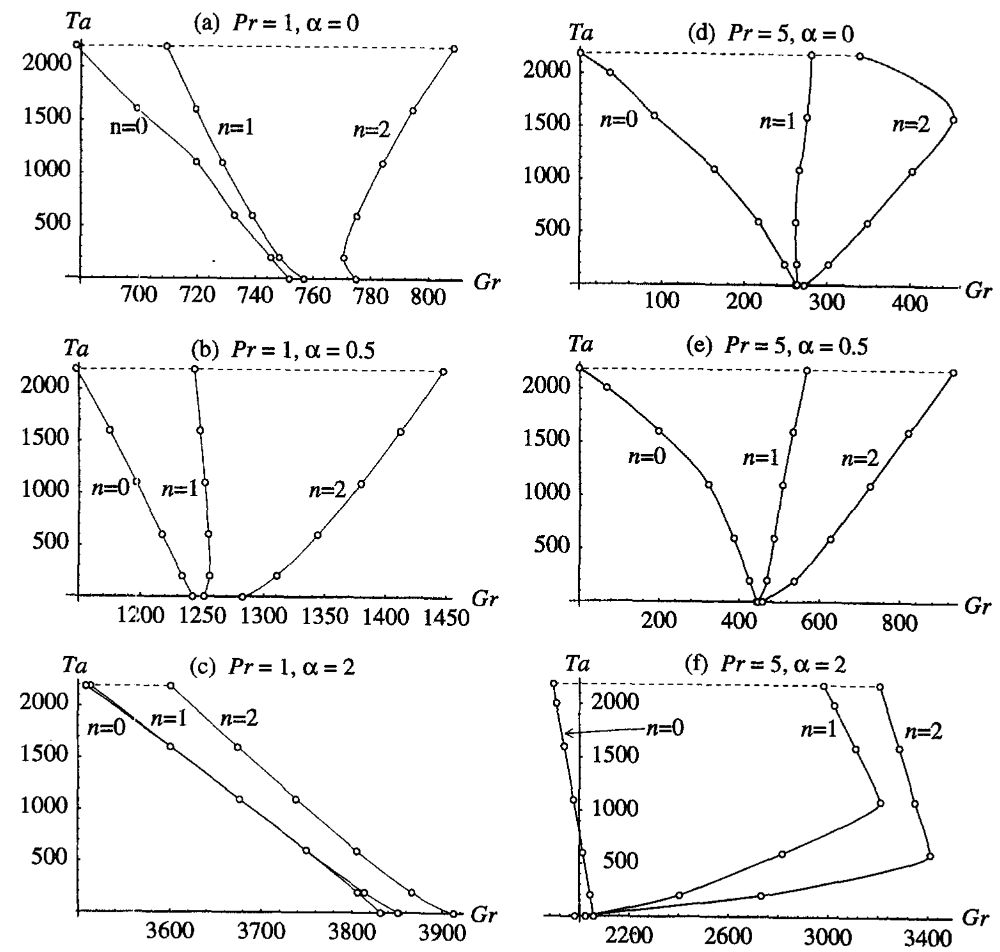

Fig. 2. Stability diagrams with $\eta = 0.7$ for $n = 0, 1, 2$, at $Pr = 1$ and (a) $\alpha = 0$, (b) $\alpha = 0.5$, (c) $\alpha = 2$, and at $Pr = 5$ and (d) $\alpha = 0$, (e) $\alpha = 0.5$, (f) $\alpha = 2$.

($n = 0$) and the first two spiral ($n = 1, 2$) modes in the case $\eta = 0.7$ and $\alpha = 0, 0.5, 2$.

In Figs. 2(a)–(c), $Pr = 1$. The case $\alpha = 0$, studied in [29], corresponds to uniform heat generation, and the results for this case are presented here and below for comparison's sake only. As seen from the figure, the axisymmetric mode is the most unstable mode for $\alpha = 0$ and $\alpha = 0.5$. Moreover, a discontinuous transition to isothermal Couette flow occurs at $Ta_c = 2186$ indicated by the dashed horizontal lines.

For $\alpha = 2$, Fig. 2(c) shows that the flow stability is determined by the concurrence of the axisymmetric and the first asymmetric modes. The flow is unstable with respect to the axisymmetric mode for small and large Taylor numbers, while the first asymmetric mode is the most unstable one for moderate values of the Taylor number. In this figure, these two modes are almost indistinguishable. Note that, in the case of radial heating, similar transitions from cellular ($n = 0$) to spiral flow and then, again, to axisymmetric cellular flow, were observed experimentally in [18] for cylinders of finite length in the case where the Grashof number was monotonically increasing.

In Figs. 2(d)–(f), $Pr = 5$. In the cases $\alpha = 0$ and $\alpha = 0.5$, the sources are uniformly, or only slightly nonuniformly, distributed; thus the axisymmetric mode is the most unstable one. Moreover, a continuous transition to isothermal Couette flow takes place in these two cases.

In the case $\alpha = 2$ [Fig. 2(f)], the mode $n = 2$ is the most unstable one at $Ta = 0$. Computations show that, without rotation, instability appears in the form of a spiral vortex moving downstream. Note that asymmetric instability in a vertical cylinder with uniform heat generation was observed experimentally in [33].

Since, in the case $Ta = 0$, the critical Grashof numbers are close to each other, we present, in the top part of Table 1, the corresponding critical values of k, Gr and c for $n = 0, 1, 2$. The critical Grashof numbers for the modes $n = 3$ and $n = 4$ are, respectively, $Gr = 2001.8$ and $Gr = 2149.7$, which are larger than the one for the mode $n = 2$. If the Taylor number increases, there is a fast transition to the axisymmetric mode, and a further increase of the Taylor number up to the critical value Ta_c, in the isothermal case, does not change the form of instability—it remains axisymmetric.

Figures 3(a)–(c) show stability curves for the larger Prandtl number, $Pr = 20$ and $\eta = 0.7$. Again, for $\alpha = 0, 0.5$ and 2, the axisymmetric mode ($n = 0$) is the most unstable mode with a continuous transition to isothermal Couette flow. The critical values of the parameters for the case $Ta = 0$ are given in the bottom part of Table 1.

Figures 3(d)–(f) show stability curves for $Pr = 1$ and $\eta = 0.4$. In this case, the flow is unstable with respect to axisymmetric modes ($n = 0$), except for very small positive values of Ta in the case $\alpha = 0.5$ where the mode $n = 1$ is the most unstable mode. In this exeptional case, the critical Grashof numbers for $Ta = 0$ are 1412.5 and 1413.7 for $n = 1$ and $n = 0$, respectively. In these figures, a discontinuous transition to isothermal Couette flow takes place as in Figs. 2(a)–(c) where $\eta = 0.7$.

In Fig. 4, the case $Pr = 5$ is characterized by the concurrence of different modes as α and Ta change. In the case of uniform internal heat sources, the flow is unstable with respect to axisymmetric perturbations [Fig. 4(a)]. If $\alpha = 0.5$ [Fig. 4(b)] the most unstable mode is the mode $n = 1$ for $Ta = 0$. This kind of asymmetric instability occurs for small positive values of Ta and, in this case, a transition to the axisymmetric mode takes place. In the case of strongly nonuniform heat sources ($\alpha = 2$) there is a sequence of transitions from the most unstable mode ($n = 2$) for $Ta = 0$, to the axisymmetric mode for large Ta [Fig. 4(c)].

Figure 4(d) is a not-to-scale magnification of the lower left-hand part of Fig. 4(c). In order to determine the stability boundary we can draw horizontal lines $Ta =$ const. and find the point of intersection, closest to the Ta-axis, of these lines and the neutral curves with $n = 0$, 1 and 2. Therefore the stability boundary of the flow in the interval $0 < Ta < 23$ (the curve DE) is determined by the spiral mode $n = 2$; the corresponding critical Grashof number varies in the interval $1774 < Gr < 2168$. Then there is a transition to the spiral mode $n = 1$ (curve EF); this mode determines the stability boundary in the rectangle $(2168 < Gr < 2985) \times (23 < Ta < 484)$. Our computations show that the values of the wave number, k, and the dimensionless phase velocity, $c = \Im$

Table 1. Critical values of k, Gr, c for $\alpha = 0, 0.5, 2$, at $Pr = 5$ (top) and $Pr = 20$ (bottom), and modes $n = 0, 1, 2$. In all cases $Ta = 0$

			$\alpha = 0$			$\alpha = 0.5$			$\alpha = 2$	
Pr	n	k	Gr	c	k	Gr	c	k	Gr	c
5	0	1.33	262.4	−1.18	1.19	443.3	−1.13	0.73	2056.7	−0.92
5	1	1.32	264.5	−1.17	1.18	446.7	−1.13	0.73	2023.7	−0.93
5	2	1.31	271.1	−1.17	1.15	457.4	−1.13	0.72	1979.3	−0.94
20	0	1.37	116.4	−1.33	1.27	193.4	−1.28	1.10	659.6	−1.06
20	1	1.37	117.2	−1.33	1.26	194.6	−1.28	1.09	660.4	−1.06
20	2	1.32	119.8	−1.32	1.24	198.1	−1.28	1.07	664.3	−1.06

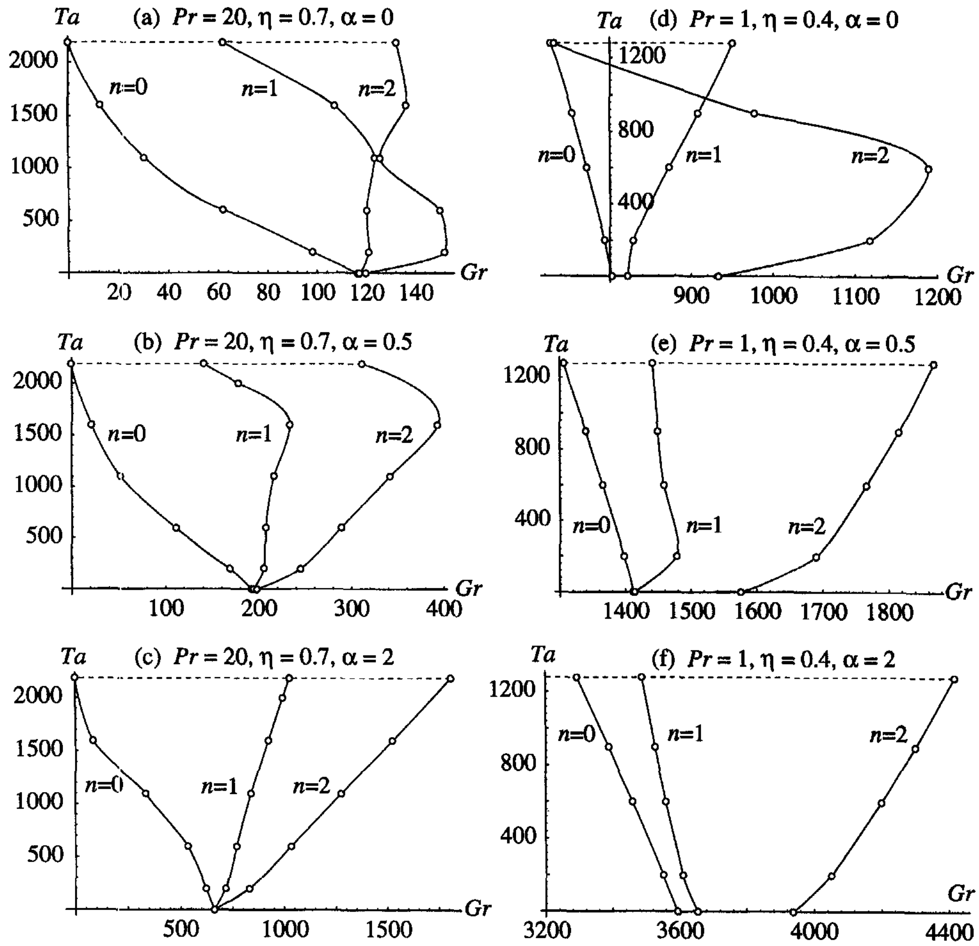

Fig. 3. Stability diagrams for $n = 0, 1, 2$, at $Pr = 20$, $\eta = 0.7$ and (a) $\alpha = 0$, (b) $\alpha = 0.5$, (c) $\alpha = 2$, and at $Pr = 1$, $\eta = 0.4$ and (d) $\alpha = 0$, (e) $\alpha = 0.5$, (f) $\alpha = 2$.

$(\lambda)/(kGrv_{0\max})$, where $v_{0\max}$ is the maximum value of the vertical component of the base velocity, are almost the same at the point E, namely, $k_2 = 0.52$, $c_2 = -0.78$, $k_1 = 0.50$, $c_1 = -0.80$ (the subscripts 2 and 1 correspond to the cases $n = 2$ and $n = 1$, respectively). If the Taylor number grows, the asymmetric instability of the mode $n = 1$ changes to the axisymmetric one ($n = 0$) at the point $(Gr, Ta) = (2985, 484)$. But, in this case, there is a jump to the axisymmetric mode, and both the wave number and the phase velocity change from $k_1 = 0.37$, $c_1 = -0.70$ to $k_0 = 1.65$, $c_0 = 0.063$. Thus, if $Ta > 484$, spiral instability changes to axisymmetric stability; the vertical sizes of the new rotating cells suddenly shrink to a vertical size close to the size of the cells for the case of isothermal Taylor vortices. Moreover, the phase velocity decreases considerably and rotating cells move slightly in the positive z-direction.

Figure 5 shows stability curves for $Pr = 20$ and $\eta = 0.4$. These curves resemble the curves of Fig. 4. The mode $n = 0$ of the flow is unstable for $\alpha = 0$.

If $\alpha = 0.5$, a transition occurs from the first asymmetric mode ($n = 1$) to the mode $n = 0$.

If $\alpha = 2$, a transition occurs from the mode $n = 2$ at $Ta = 0$, with $k_2 = 0.77$, $c_2 = -0.83$, to the mode $n = 1$ at the point $(Gr, Ta) = (761, 29)$, with $k_1 = 0.82$, $c_1 = -0.86$. A further transition occurs from the mode $n = 1$, with $k_1 = 0.80$, $c_1 = -0.83$, to the mode $n = 0$ at the point $(Gr, Ta) = (799, 70)$, with $k_0 = 0.95$, $c_0 = -0.87$. If $Pr = 20$, the Ta-interval of flow instability with respect to an asymmetric mode is narrower than in the case $Pr = 5$ (see Fig. 4). We also note that there is only a small jump in the values of k and c at the transition.

It can be seen from Figs. 2–5, that, in all cases, the axisymmetric mode ($n = 0$) corresponds to flow destabilization (Ta decreases as Gr increases), and, on the other hand, in many cases, the asymmetric modes ($n = 1$, 2) correspond to flow stabilization (Ta increases as Gr increases). For small Prandtl numbers [see, for example, Figs 2(a)–(c)], stabilization will not be observed experimentally: the critical Taylor numbers for asymmetric modes are higher then those for axisymmetric modes. However, an increase of the Prandtl number ($Pr = 5$ and $Pr = 20$ in our computations) leads to the appearance of regions of sta-

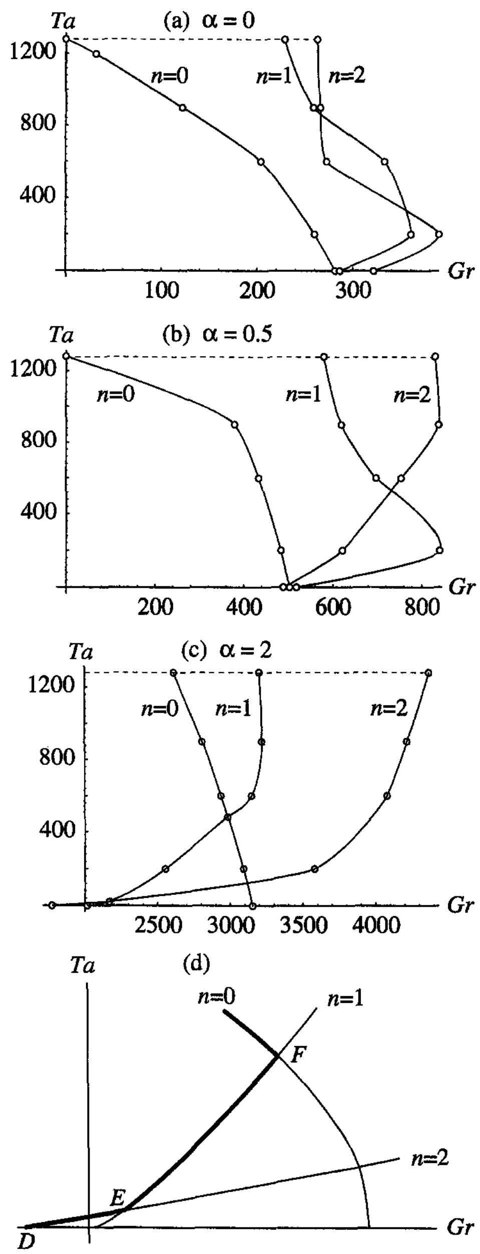

Fig. 4. Stability diagrams for $Pr = 5$, $\eta = 0.4$, $n = 0, 1, 2$; (a) $\alpha = 0$, (b) $\alpha = 0.5$, (c) $\alpha = 2$. (d) Not-to-scale magnification of lower left-hand part of (c) (see text).

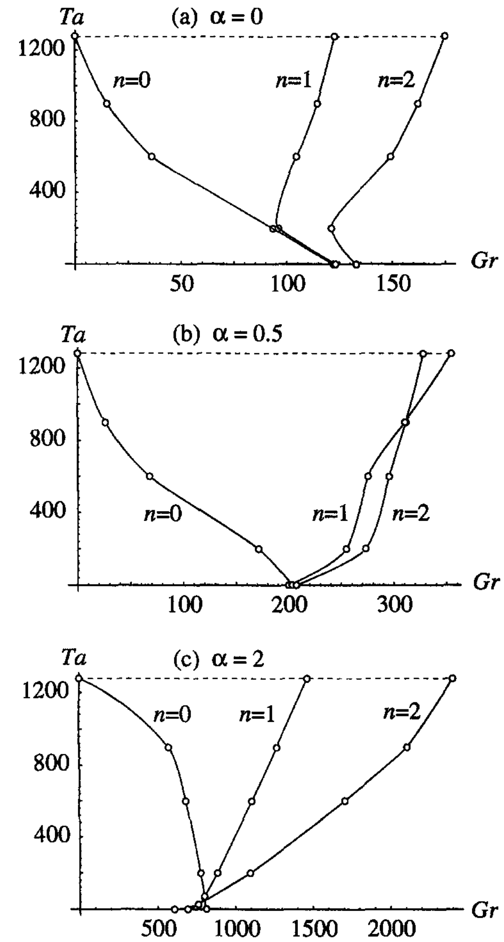

Fig. 5. Stability diagrams for $Pr = 20$, $\eta = 0.4$, $n = 0, 1, 2$; (a) $\alpha = 0$, (b) $\alpha = 0.5$, (c) $\alpha = 2$.

bilization [see, for example, curve DF in Fig. 4(d)] which can be observed experimentally. Moreover, as previously mentioned, stabilization of Couette flow by radial heating was observed experimentally [16].

Stabilization for large α can be explained in the following way. According to equation (1), for large α the density of heat sources decreases rapidly in the positive radial direction. In other words, heat sources are concentrated near the inner cylinder and the temperature distribution becomes close to the case of radial heating with negative temperature gradient, i.e. heated inner cylinder and cooled outer cylinder. This negative temperature gradient stabilizes the flow since the lighter fluid particles near the heated inner cylinder have a smaller centrifugal force exerted on them. This fact was confirmed for narrow gaps experimentally in [14] and theoretically in [17].

We have also shown that the region of stabilization decreases as the Prandtl number increases. This fact was also found in [29] but for very wide gaps ($\eta = 0.1$). Note that asymmetric instabilities and the stabilization of Couette flow by a positive density gradient were also observed experimentally in [34, 35].

4. CONCLUSION

The stability of a flow, between a rotating inner cylinder and a stationary outer cylinder, in the presence of nonuniformly distributed heat sources, is studied in this paper for wide gaps ($\eta = 0.7$ and $\eta = 0.4$). It is found that if the nonuniformity of the heat sources is small ($\alpha = 0.5$), the instability is mainly of an axisymmetrical nature and the critical Grashof number decreases as the Taylor number grows. On the other hand, in the case of strongly nonuniform heat sources

($\alpha = 2$) there exist regions of stabilization of Couette flow. These regions correspond to instability of asymmetric type. As the Grashof number grows, there exists a sequence of transitions from the asymmetric mode $n = 2$ to the axisymmetric mode $n = 0$.

Acknowledgements—This work was supported in part by the Natural Sciences and Engineering Research Council of Canada under grant A7916, and the Centre de Recherches Mathématiques of the Université de Montréal. The authors gratefully acknowledge the contribution of the reviewer who found a misquote in a previous version of this paper.

REFERENCES

1. G. I. Taylor, Stability of a viscous fluid contained between two rotating cylinders, *Phil. Trans. R. Soc. Lond. A* **223**, 289–343 (1923).
2. R. C. DiPrima and H. L. Swinney, Instabilities and transition in flow between concentric rotating cylinders, In *Hydrodynamic Instabilities and Transition to Turbulence* (Edited by H. L. Swinney and J. P. Gollub), Topics in Applied Physics, Vol. 45, pp. 139–180. Springer, New York (1981).
3. J. T. Stuart, Taylor vortex flow: a dynamical system, *SIAM Review* **28**, 315–342 (1986).
4. R. M. Lueptow, A. Docter and K. Min, Stability of axial flow in an annulus with a rotating inner cylinder, *Phys. Fluids A* **4**, 2446–2455 (1992).
5. Jyh-Chen Chen and Jer-Yow Kuo, The linear stability of steady circular Couette flow with small radial temperature gradient, *Phys. Fluids A* **2**, 1585–1591 (1990).
6. Kai-Hsiung Kao and Chuen-Yen Chow, Linear stability of compressible Taylor–Couette flow, *Phys. Fluids A* **4**, 984–996 (1992).
7. F. F. Hatay, S. Biringen, G. Erlebacher and W. E. Zorumski, Stability of high-speed compressible rotating Couette flow, *Phys. Fluids A* **5**, 393–404 (1993).
8. M. Ali and P. D. Weidman, On the linear stability of cellular spiral Couette flow, *Phys. Fluids A* **5**, 1188–1200 (1993).
9. M. Ali and P. D. Weidman, On the stability of circular Couette flow with radial heating, *J. Fluid Mech.* **220**, 53–84 (1990).
10. L. S. Yao and B. B. Rogers, Finite-amplitude instability of non-isothermal flow in a vertical annulus, *Proc. R. Soc. Lond. A* **437**, 267–290 (1992).
11. B. B. Rogers, S. G. Moulic and L. S. Yao, Finite-amplitude instability of mixed convection, *J. Fluid Mech.* **254**, 229–250 (1993).
12. G. B. McFadden, S. R. Coriell, B. T. Murray, M. E. Gliksman and M. E. Selleck, Effect of a crystal–melt interface in a Taylor vortex flow, *Phys. Fluids A* **2**, 700–705 (1990).
13. J. Kaye and E. C. Elgar, Modes of adiabatic and diabatic fluid flow in an annulus with an inner rotating cylinder, *Trans. ASME C: J. Heat Transfer* **80**, 753–765 (1958).
14. K. M. Becker and J. Kaye, The influence of a radial temperature gradient on the instability of fluid flow in an annulus with an inner rotating cylinder, *Trans. ASME C: J. Heat Transfer* **84**, 106–110 (1962).
15. J. Walowit, S. Tsao and R. C. DiPrima, Stability of flow between arbitrarily spaced concentric cylinder surfaces, including the effect of a radial temperature gradient, *Trans. ASME E: J. Appl. Mech.* **31**, 585–593 (1964).
16. H. A. Snyder and S. K. F. Karlsson, Experiments on the stability of Couette motion with a radial temperature gradient, *Phys. Fluids* **7**, 1696–1706 (1964).
17. K. S. Ball and B. Farouk, Bifurcation phenomena in Taylor–Couette flow with buoyancy effects, *J. Fluid Mech.* **197**, 479–501 (1988).
18. K. S. Ball and V. C. Dixit, An experimental study of heat transfer in a vertical annulus with a rotating inner cylinder, *Int. J. Heat Mass Transfer* **32**, 1517–1527 (1989).
19. J. C. Patterson, Unsteady natural convection in a cavity with internal heating and cooling, *J. Fluid Mech.* **140**, 135–151 (1984).
20. M. J. Coates and J. C. Patterson, Unsteady natural convection in a cavity with non-uniform absorbtion of radiation, *J. Fluid Mech.* **256**, 133–161 (1993).
21. F. Chen and A. J. Pearstein, Hot spot locations and temperature distributions in a forced convection photochemical reactor, *Int. J. Heat Mass Transfer* **36**, 2105–2114 (1993).
22. H. O. May, A numerical study of natural convection in an inclined square enclosure containing internal heat sources, *Int. J. Heat Mass Transfer* **34**, 919–928 (1991).
23. E. R. Cooper, D. F. Jankowski, G. P. Neitzel and T. H. Squire, Experiments on the onset of instability in unsteady circular Couette flow, *J. Fluid Mech.* **161**, 97–113 (1985).
24. G. Z. Gershuni, E. M. Zhukhovitskii and A. A. Iakimov, On the stability of steady convective motion generated by internal heat sources, *Sov. J. Appl. Math. Mech.* (English Transl.) **31**, 669–674 (1970).
25. G. Z. Gershuni, E. M. Zhukhovitskii and A. A. Iakimov, Two kinds of instability of stationary convective motion induced by internal heat sources, *Sov. J. Appl. Math. Mech.* (English Transl.) **34**, 544–548 (1973).
26. V. M. Shikhov and V. I. Yakushin, Stability of convective motion caused by inhomogeneously distributed internal heat sources, *Fluid Dyn.* (English Transl.) **12**, 457–461 (1977).
27. A. A. Kolyshkin and R. Vaillancourt, Stability of internally generated thermal convection in a tall vertical annulus, *Can. J. Phys.* **69**, 743–748 (1991).
28. A. A. Kolyshkin and R. Vaillancourt, On the stability of convective motion caused by inhomogeneous internal heat sources, *Arabian J. Sci. Engng* **17**(4B), 655–662 (1992).
29. A. A. Kolyshkin and R. Vaillancourt, On the stability of nonisothermal circular Couette flow, *Phys. Fluids A* **5**, 3136–3146 (1993).
30. A. A. Kolyshkin and R. Vaillancourt, A note on a method of solution for convective stability problems, *Comm. Appl. Numer. Methods* **5**, 299–307 (1989).
31. B. B. Rogers and L. S. Yao, The importance of Prandtl number in mixed-convection instability, *Trans. ASME C: J. Heat Transfer* **115**, 482–486 (1993).
32. M. Prud'homme, L. Robillard and M. Hilal, Natural convection in an annular fluid layer rotating at weak angular velocity, *Int. J. Heat Mass Transfer* **36**, 1529–1539 (1993).
33. V. G. Kozlov and N. G. Polyakova, Stability of convective motion in a vertical circular channel caused by internal heat sources, In *Convective Motions and Hydrodynamic Instability*, pp. 24–28. Sverdlovsk, UNC Akad. Nauk SSSR (1979) (in Russian).
34. E. M. Withjack and C. F. Chen, An experimental study of Couette instability of stratified fluids, *J. Fluid Mech.* **66**, 725–737 (1974).
35. S. R. M. Gardiner and R. H. Sabersky, Heat transfer in an annular gap, *Int. J. Heat Mass Transfer* **21**, 1459–1466 (1978).